Future Foods 12 (2025) 100844

Contents lists available at ScienceDirect

Future Foods

journal homepage: www.elsevier.com/locate/fufo

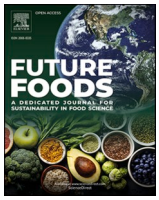

Design of an innovative fiber-rich spreadable cheese up-cycling olive stones: structural and sensory characterization

Niccolò Renoldi [a], Federico Basso [a], Francesca Trevisiol [a], Hana Maalej [b], Nadia Innocente [a,*], Sonia Calligaris [a]

[a] Department of Agricultural, Food, Environmental and Animal Sciences, University of Udine 33100, Udine, Italy
[b] University of Gabes, Faculty of Sciences of Gabes, Laboratory of Biodiversity and Valorization of Arid Areas Bioresources (BVBAA), LR16ES36, Faculty of Sciences, Erriadh 6072, Gabes, Tunisia

ARTICLE INFO

Keywords:
Functional cheese
Dietary fiber
By-product
Valorization
Olive stones
Cheese structure
Caseins

ABSTRACT

The olive industry generates annually huge quantities of by-products, including olive stones (OS) which are currently used almost exclusively for energy production through combustion. However, OS could be considered a source of dietary fibers, thus opening the possibility to design alternative valorization pathways in a circular-economy perspective. To explore this potential, OS (81 % fiber) were locally collected, dried, and milled (particle size < 0.5 mm). The resulting OS powder was then incorporated into a model spreadable cheese formulation before curding, at concentrations of 3.5 and 7.0 g/100 g, to meet the "source of fiber" and "high in fiber" nutritional claims, respectively. The addition of OS induced a significant change in the visual appearance, with an overall darkening of the matrix, without affecting its moisture content. Regarding structural properties, OS inclusion at both levels significantly improved the spreadability of cheese, while reducing its elastic properties compared to the control. Confocal microscopy revealed OS fibers affected the microstructure of the typical three-dimensional protein network present in the curd, with large insoluble fiber particles embedded in protein aggregates and acting as inactive fillers. Sensory analysis showed that consumer acceptability remained high, although it declined with increasing OS content. These findings demonstrate that incorporating OS powder at 3.5 g/100 g into innovative spreadable cheese is technologically feasible and nutritionally beneficial, offering a new way for the valorization of OS as a healthy functional food ingredient.

1. Introduction

Nowadays, the consumption of dietary fiber-rich foods plays a crucial role in promoting digestive health, weight management, and reducing the risk of chronic conditions such as heart disease, diabetes, and certain types of cancer (Anderson et al., 2009; Zhao et al., 2018). In particular, due to their chemical structure and low density, they can increase fecal bulk, lumen viscosity, and decrease intestinal transit through promotion of the digestive system movement, as well as benefit gastrointestinal microbiota as prebiotic ingredients (Mudgil, 2013). The international food safety agencies set the recommended daily fiber intakes between 25 and 34 g/day, based on country of residence, gender, and age, to ensure physiological benefits to the consumer (EFSA, 2016; Trumbo et al., 2002).

Unfortunately, the vast majority of food products consumed worldwide on a daily basis typically lack these compounds, that are mainly present in fruits, vegetables, whole grains, and legumes (Borneoand León, 2012; Brummer et al., 2015; Slavin and Lloyd, 2012). For this reason, an increasing number of product categories are being today fortified with dietary fibers to enhance their nutritional profile and health promoting capacity properties.

An interesting food category for fiber enrichment is represented by dairy products, which are consumed by a large portion of the population, therefore representing strategic foods to impact public health through dietary fiber consumption. However, fiber enrichment of dairy formulations has been sporadically explored in literature, with particular reference principally to ice cream, yogurt and fermented milk, and milk-based beverages (Gomes et al., 2023; Rezvani and Goli, 2024; Tian et al., 2024; Tolve et al., 2024). Incorporating dietary fiber from plant-based sources into these dairy products mainly resulted in an increase of the nutritional profile of the products. However, the presence of fibers could alter the structure and especially the microstructure of

* Corresponding author at: Department of Agricultural, Food, Environmental and Animal Sciences, University of Udine, Via Sondrio 2/A 33100, Udine, Italy.
E-mail address: nadia.innocente@uniud.it (N. Innocente).

https://doi.org/10.1016/j.fufo.2025.100844
Received 4 September 2025; Received in revised form 14 November 2025; Accepted 15 November 2025
Available online 16 November 2025

the system. In dairy products like ice cream and yogurt, incorporation of dietary fiber led to an increase of matrix viscosity, reducing syneresis over time (Dewi et al., 2025). On the other hand, a structural softening in enriched spreadable cheeses was reported by Gammariello et al. (2008) and Difonzo et al. (2024) after the incorporation of chitosan and xylooligosaccharides extract, respectively. These compounds disrupted the typical protein network, leading to structural changes that ultimately resulted in lower product overall acceptability (Gammariello et al., 2008). More in-depth studies are needed to better understand the effect of dietary fiber on the microstructure of dairy products, since only a few data have been reported on the interactions between fiber and casein networks (Fagan et al., 2006; Maroziene and De Kruif, 2000).

Considering the urgent need to increase the daily dietary fiber intake, the identification of alternative fiber-rich sources may be strategic, since a significant portion of dietary fibers is lost as waste during food processing, representing an underutilized resource with potential for valorization. Industrial waste and by-products generated by the agri-food sector might represent an innovative possibility to identify alternative sources of dietary fiber, also enhancing the processing of sidestreams within a circular economic perspective. In this context, considering their substantial annual production, olive stones (OS) generated during the milling of olives for the production of olive oils could be of particular relevance. The olive industry is one of the major industries in the Mediterranean region and OS contribute globally to the generation of approximately 4 to 5 million tons of waste needing a well-defined strategic plan for sustainable and green re-use (Bai et al., 2023). This under-exploited by-product is currently used almost exclusively for energy production through combustion (García Martín et al., 2020). However, OS are characterized by high levels of dietary fiber, with values ranging from 53.2 % to 74.5 % (Bolek, 2020; Jahanbakhshi and Ansari, 2020; Oncel and Ozbek, 2025). Dietary fiber in OS mainly consists of insoluble lignocellulosic material, including cellulose (20–40 %), lignin (25–35 %), and hemicellulose (18–32 %) (Soares et al., 2024). Moreover, OS contain also a wide range of polyphenols and flavonoids with potential antioxidant activity, thus increasing the attractiveness of this by-product (Bolek, 2020; Hannachi et al., 2020). For these reasons and based on OS high fiber content, a promising application of such by-product of the olive supply chain could be as a functional ingredient for promoting health through fiber enrichment of dairy food formulations. To the best of our knowledge, there are no studies in the scientific literature on the incorporation of OS in dairy products. Therefore, this study aimed to evaluate the feasibility of OS as fiber enriching ingredient in spreadable cheese products. Exploitability of OS powder in experimental samples was measured in terms of its impact on physico-chemical, structural, and sensorial properties.

2. Materials and methods

2.1. Olive stone powder preparation

Olive stones (OS) were kindly supplied by the Consortium of Extra Virgin Olive Oil Producers of Friuli Venezia Giulia (Udine, Italy), after the October 2024 olive harvest. Stones were mechanically separated during the extraction process of extra virgin olive oil, collected immediately after milling in a food-grade manner in plastic bags, and stored at −18 °C until use. For the preparation of the powder, the stones were firstly thawed at room temperature for 2 h, and then oven dried (Memmert, Schwabach, Germany) at 40 °C for 2 h to remove excessive moisture and avoiding powder collapse. Dried stones were then ground using a ball mill (MM 500 Vario, Haan, Germany) at a frequency of 25 Hz for 2 min and sieved to achieve a particle size lesser than 0.5 mm. The resulting OS powder was stored in vacuum-sealed plastic bags.

2.2. Production of spreadable cheeses

Spreadable cheese samples were prepared following the method described by Rinaldoni et al. (2014) with few modifications. Each sample was manufactured in a multifunction kitchen robot (Moulinex, France) equipped with a 3 L vat. Different concentrations of OS powder, including 0, 7, and 14 g/L, were separately added to 1 L of partially skimmed cow milk (1.5 % of fat, 3.3 % of protein) (Despar, Udine, Italy) to achieve fiber levels corresponding to the European health claims of "source of fiber" (≥3 g/100 g) and "high in fiber" (≥6 g/100 g), listed by the European Commission within the Regulation No 1924/2006 (European Parliament and Council, 2006). For cheese production, the milk was heated at 85 ± 2 °C for 10 min under constant stirring. Once cooled down to 25 °C, the pH was adjusted to 4.6 using a citric acid solution (40 g/100 mL) (Sigma Aldrich, Italy), and 0.4 g of $CaCl_2$ (Sigma Aldrich, Italy) were added. The mixture was then treated in a water bath at 70 ± 2 °C for 60 min. After this second heating step, the curd was filtered and recovered, while the whey was discarded. The curd was then homogenized with 0.5 g of NaCl (Sigma Aldrich, Italy) at 500 rpm for 20 s using the kitchen robot. Samples were transferred to glass containers and stored at 4 °C overnight before analysis.

2.3. Analytical determinations

2.3.1. OS chemical characterization

The chemical composition of OS and cheese samples was analyzed using the reference AOAC methods and IDF standard procedures (IDF, 2021), respectively. In particular, moisture content was determined following the AOAC gravimetric method (AOAC, 2005). Total lipids of OS powder were quantified via Soxhlet extraction (AOAC, 2005), while the fat content in cheeses was determined following the official IDF gravimetric method (IDF, 2022). Soluble and insoluble dietary fibre were assessed with a total dietary fibre assay kit (TDF-100A, Sigma Aldrich, St. Louis, Missouri, USA) (AOAC, 2011). Total protein content of OS was calculated using the Kjeldahl method (AOAC, 2005), while in cheese samples was used the IDF method for nitrogen fractions (IDF, 2011). The ash content was calculated by incinerating approximately 10 g of the sample at 550 °C (RO-8, Gossen Metrawatt, Nürnberg, Germany) (AOAC, 1923). Carbohydrates were obtained by difference with the other components.

2.3.2. OS particle size distribution

The particle size distribution of the OS powder was measured by laser scattering diffraction using a Mastersizer 3000+ (Malvern Instruments, Malvern, UK). Measurements were performed in deionized water with a laser obscuration of 10 % and an agitation speed of 2500 rpm. The refractive indices of the powder and water were set at 1.580 and 1.330, respectively, while the particle absorption index was 0.010.

2.3.3. OS bulk density

The bulk density of OS was calculated by determining the volume of 1.5 g of powder in a graduated syringe, gently tapped, and reported in g cm^{-3} (Manzocco et al., 2024).

2.3.4. OS water and oil holding capacities

Distilled water or sunflower oil (1 g) was added to OS (0.04 g), and the suspensions were stirred for 30 s using a vortex (Vortex 1, Ika, Milan, Italy). After resting for 15 min, the samples were centrifuged (Mikro 120, Hettisch, Milan, Italy) at 20,000 × *g* for 20 min at 4 °C. The supernatant was then removed, and the precipitate was weighed. Water holding capacity (WHC, %) and oil holding capacity (OHC, %) were calculated as reported by Renoldi et al. (2023).

2.3.5. Water activity

Water activity (a_w) of OS and cheese samples was measured at 25 °C using an AquaLab Series 4TE (Decagon Devices, Pullman, Washington, USA).

2.3.6. Color

Color analysis of OS and cheeses was performed using a tristimulus colorimeter (Chromameter-2 Reflectance, Konica Minolta, Japan) equipped with a CR-400 measuring head and illuminant "C" (6774 K). Samples were placed in Petri dishes and a minimum of five measurements were taken for each sample. The color was expressed using the CIE L*, a*, b* chromatic parameters.

2.3.7. pH of samples

A pH meter (Basic 20, Crison, Spain), previously calibrated with standard solutions at pH values of 4, 7, and 9, was used to evaluate the pH of adequately diluted OS powder and cheese-water dispersions.

2.3.8. Syneresis

Syneresis of samples was determined following the method described by Rinaldoni et al. (2014) with few modifications. Approximately 0.5 g of each sample was centrifuged at 10,000 × *g* for 20 min at 4 °C (Mikro 120, Hettisch Italia srl, Milan, Italy). The degree of syneresis (DS) was calculated (Eq. (1)) as the amount of whey separated from the cheese after centrifugation, related to the total mass of the centrifuged sample:

$$\mathrm{DS}\ (\mathrm{g}/100\mathrm{g}) = (\mathrm{massofwhey}/\mathrm{massofcheese}) \times 100 \quad (1)$$

2.3.9. Image acquisition

Digital images of samples were captured using a professional camera Canon reflex (EOS 550D, Canon Inc., Tokio, Japan) equipped with an EF-S 60 mm f/2.8 Macro USM lens, and with a resolution of 550 dots per inch. The camera was positioned 30 cm away from the samples, inside a photography booth with a black background (Images and Computer, Bareggio, Italy).

2.3.10. Determination of rheological parameters

Viscoelastic properties were determined using a controlled-stress rotational rheometer (Haake RheoStress 6000, ThermoScientific, Karlsruhe, Germany) equipped with a temperature-controlled system. Measurements were performed at 25 °C, using serrated plates with a diameter of 35 mm and a 2 mm gap. After relaxing for 5 min, a stress sweep test was carried out within the 0.1–1000 Pa domain to identify the linear viscoelastic range (LVR). Frequency sweep tests were performed from 0.1 to 10 Hz within the LVR at a constant shear stress (5 Pa). Storage modulus (G'), loss modulus (G''), loss tangent (tan δ = G''/G'), and complex viscosity (η*) were measured and then compared at 1 Hz.

2.3.11. Evaluation of mechanical properties

Mechanical properties of cheese samples were evaluated by performing texture profile analysis (TPA) and spreadability tests, according to Bayarri et al. (2012). Both analyses were conducted using a universal dynamometer (Instron 34TM-5, USA) equipped with a 5 kN load cell. Prior to analysis, samples were conditioned at 18 ± 1 °C for one hour to ensure thermal equilibrium and standardization.

For TPA compressions, a circular probe with a 45 mm diameter and a speed test of 4 mm/s was used. Cheese cylinders (36.5 mm diameter and 31.2 mm height) were prepared and centrally placed on the lower plate of the instrument. The test involved two consecutive uniaxial compressions (30 % deformation) with a 5-second interval between compressions to mimic mastication. Attributes such as hardness (N), elasticity, adhesiveness (N), gumminess, and cohesiveness were obtained from the force-time curve.

For spreadability, a conical probe with 51 mm diameter and 33 mm height was used to compress samples with a speed test of 1 mm/s for up to 20 mm. Samples were inserted inside holders matching the angle of the conical probe paying attention not to form air pockets, and their surface was levelled using a kitchen spatula before analysis. The force opposed by the samples to the penetration of the probe was recorded as a function of time, and the relevant curves were elaborated using OriginPro 2021 (OriginLab, Northampton, MA, USA). In particular, curves were integrated to obtain the total underlying area and the maximum force, and were subsequently fitted with a power-law model as reported in Eq. (2).

$$Force = a + bt^c \quad (2)$$

Where *a* (N) indicates the break-off force perceived by the instrument at the beginning of the analysis, *b* (N s^C) is the scaling parameter reflecting the magnitude of the force increase during the analysis, and *c* is a dimensionless exponent describing the shape of the force curve, as previously described by Faber et al. (2017) and Leach et al. (2003).

2.4. Confocal laser scanning microscopy (CLSM)

Microstructural images were acquired using a laser scanning confocal microscope (TCS SP8 X, Leica Microsystems, Germany) equipped with a Leica HC PL FLUOTAR 10x/0.3 NA dry objective. For analysis, 0.5 g of each sample was mixed with 17 μL of the respective dyes - Nile Red, Fast Green FCF, and Brightener - used to visualize lipids, proteins and fibers, respectively. A small amount of dyed sample was then deposited on a glass slide and covered with coverslip. Transparent nail polish was then applied on the corners of the coverslip to fixate it and prevent sample moisture loss during analysis. The excitation and detection wavelengths for the dyes used were as follows: (i) Nile Red: excitation at 535 nm, detection 545–585 nm; (ii) Fast Green FCF: excitation 630 nm, detection 640–705 nm; (iii) Brightener: excitation 405 nm, detection 415–480 nm. Images were finally elaborated using LasX v3.5.5 (Leica Microsystems).

2.5. Sensory analysis

A heterogeneous group of 43 habitual spreadable cheese consumers was recruited for the acceptability test. Before analysis, samples were incubated at 18 °C and labeled with randomized three-digit codes. Each sample was presented individually in a randomized order, and participants were asked to rate five sensory attributes: visual appearance, odor, taste, mouthfeel, and overall acceptability. Ratings were recorded using a 9-point hedonic scale (1 = "unacceptable" to 9 = "fully acceptable"). Participants were provided with crackers and still water to cleanse their palate between samples. Sessions were conducted in individual booths illuminated by standard white light to minimize external influences. Data collection and analysis was performed using the Smart Sensory Box version 2.2.44 software (Smart Sensory Box, Sassari, Italy).

The study complied with the principles established by the Declaration of Helsinki and the protocol was approved by the Institutional Review Board of the Department of Agricultural, Food, Environmental and Animal Sciences of the University of Udine (protocol n. 0154,557).

2.6. Statistical analysis

All analyses were conducted in triplicate on three independent samples except for microstructure and sensory testing. All numerical data were reported as mean ± standard deviation. Data characterized by homoscedastic variance (Bartlett test, $p = 0.05$) were compared using one-way analysis of variance (ANOVA, $p = 0.05$) followed by Tukey's HSD test, whereas data with dishomogeneous variance were subjected to non-parametric Kruskal-Wallis ANOVA ($p = 0.05$) followed by Dunn test ($p = 0.05$) to obtain data ranking and enable compact letter display. Statistical analysis was performed using OriginPro 2021 (OriginLab, Northampton, MA, USA).

3. Results and discussion

3.1. Proximate composition and technological properties of OS

The proximate composition and the physicochemical characteristics

of OS, obtained by drying and milling the original olive stones, are provided in Table 1.

As expected, the predominant component of the OS was represented by insoluble dietary fibers (89 g/100 g of dry matter), followed by carbohydrates, in line with literature (Oncel and Ozbek, 2025). Lipid and protein represented a minor portion below 1.5 g/100 g of dry matter. Bolek (2020) and Jahanbakhshi and Ansari (2020) previously found that the chemical composition of OS can vary depending on cultivar, stones separation method, and oil extraction process. The OS powder was made of fine particles, mainly composed of particles with a diameter in the range of 300–500 μm, followed by particles with a diameter between 200 and 300 μm, representing around 25 %. As expected, the water activity of OS was low (0.25 ± 0.01), due to the low moisture content (Table 1). A low a_w value is important to reduce susceptibility to microbial growth, enhancing OS stability during storage. Moreover, the OS exhibited an apparent density of approximately 0.73 g/cm^3. This value is slightly higher than those of other lignocellulosic biomasses, such as date stones powder, which has a bulk density of 0.32 g/cm^3, and wood from *Pinus oocarpa*, which has a bulk density of 0.48 g/cm^3 (Bouchelta et al., 2008; de Oliveira Menali et al., 2024). Bulk density values are strongly influenced by the structural properties of the matrices (Heuscher et al., 2005). Compared to other lignocellulosic materials, OS of this study resulted in a more closely packed structure with low porosity. This is the reason probably for the low WHC and OHC values (Table 1), indicating a reduced capacity of the powder to interact with the common solvents in food products, such as water and oil. Finally, the colorimetric analysis of OS reveals a high value of lightness (L*) with a slight red hue (a*) and a pronounced yellow component (b*) (Table 1), resulting in an overall brown appearance.

3.2. Physicochemical properties of OS-enriched spreadable cheese

The effect of OS addition on the visual appearance and physicochemical properties of spreadable cheese was initially evaluated (Table 2).

As clearly shown by the data reported in Table 2, the addition of OS induced a significant change in visual appearance, with particular reference to a grainier surface showing a reduced occurrence of holes and cracks. Besides allowing a better maintenance of cheese shape upon shearing and spreading, the addition of OS also caused a slight darkening of the matrix, which was analytically confirmed by the significant decrease in L* and increase of a* and b* chromatic coordinates (Table 2). Color changes in enriched products were mainly attributed to the presence of brown-yellowish insoluble particles clearly visible to the naked eye and highlighted also in Table 1. Difonzo et al. (2024) observed a similar trend in cheese color modification after the addition of xylooligosaccharides extract, due to the presence of dark pigments and other natural fractions. Different from visual appearance and color, adding OS to the cheese formulation caused no significant changes in the moisture content, with only minor fluctuations in water activity values (Table 2). As expected, the addition of 3.5 and 7 g/100 g OS powder significantly increased the total dietary fiber content of cheeses (Table 2), allowing experimental samples to meet the criteria for "source of fiber" and "high in fiber" nutritional claims, respectively. The fiber-enriched cheese samples exhibited an apparent reduction in protein, fat, carbohydrates, and ash contents compared with the control. These differences are not likely attributable to losses of these components into the whey as a consequence of structural modifications in the casein matrix. Instead, they can be reasonably explained by a mass balance effect: when dietary fiber is added, it contributes to the total solid content, so that the relative proportion of the other constituents decreases accordingly. With regard to carbohydrates, in the control sample these are represented exclusively by lactose, whereas in the fiber-enriched samples, they also include the carbohydrate fraction originally present in OS powder (accounting for approximately 8 % of the OS powder dry matter). The pH in OS-enriched samples slightly increased ($p < 0.05$, ANOVA) in comparison with the control sample, probably because of the high pH value of the OS powder (Table 1). No significant differences were found between samples containing OS powder, suggesting a buffering effect of this ingredient. The pH of cheese plays a crucial role in shaping its structural and rheological properties. Variations in pH can alter protein–water interactions, thereby affecting the compactness of the final product (Monteiro et al., 2009). Moreover, water retention during storage is another critical parameter that directly reflects the structural stability of cheese (Rinaldoni et al., 2014). All cheese formulations showed comparable syneresis values ($p > 0.05$, ANOVA) after centrifugation (Table 2), indicating that although OS addition may influence the protein network, the low water-holding capacity of fibers (Table 1) allowed effective water retention and prevented undesired loss of whey. Based on these results, the attention was focused on the effect of OS addition on the mechanical and rheological properties of the spreadable cheese.

Table 1
Proximate composition and physicochemical characteristics of the OS powder.

Parameter	OS powder
Moisture (g/ 100 g wm)	9.80 ± 0.14
Lipid (g/ 100 g dm)	0.44 ± 0.04
Fiber (g/100 g dm)	90.02 ± 0.15
Insoluble (g/100 g dm)	89.56 ± 0.10
Soluble (g/100 g dm)	0.45 ± 0.03
Protein (g/100 g dm)	0.86 ± 0.01
Carbohydrate* (g/100 g dm)	8.51 ± 0.06
Ashes (g/100 g dm)	0.19 ± 0.01
Particle size (%)	
< 100 μm	16.06 ± 0.40
100 < x < 200 μm	16.27 ± 0.96
200 < x < 300 μm	24.80 ± 0.27
300 < x < 500 μm	42.87 ± 1.61
a_w	0.25 ± 0.01
pH	7.14 ± 0.01
Bulk density (g/cm^3)	0.73 ± 0.04
OHC (g_{oil}/g_{dm})	1.60 ± 0.20
WHC (g_{water}/g_{dm})	1.70 ± 0.10
Color	
L*	79.3 ± 1.2
a*	5.3 ± 0.2
b*	22.7 ± 0.4

wm: wet matter; dm: dry matter. *obtained by difference from other components.

3.3. Rheological and mechanical properties

Rheological analyses were performed to extrapolate information regarding the effect of OS addition on the small-stress mechanical response of spreadable cheese. To this end, frequency sweep analysis was carried out applying stress values within the linear viscoelastic region (Fig. 1).

Rheological test clearly revealed a weak gel-like behavior for all samples, showing a linear frequency-dependence for both the elastic and the viscous moduli in the entire oscillatory frequency domain considered (Fig. 1). Moreover, rheological profiles indicated that the incorporation of OS in the formulation did not alter the rheological behavior of the samples, as no change in the frequency dependence of both moduli was observed in samples containing 3.5 and 7 g/100 g OS as compared to the control ones. In addition, in all samples the storage modulus (G') was above the loss modulus (G'') in the entire frequency range, indicating that the elastic response prevailed on the relative viscous counterpart typical of viscoelastic structures (Rao and Steffe, 1992). Similar rheological behaviors were reported by Rinaldoni et al. (2014) and Gammariello et al. (2008) for spreadable cheese-like products enriched with soy protein concentrates and chitosan dietary fiber, respectively.

Based on the data reported in Table 3, it can be observed that the

Table 2
Visual appearance, color, moisture content, water activity (a_w), pH and syneresis of spreadable cheese samples containing increasing amounts (0–7 g/100 g) of OS powder.

Parameter		OS powder content (g/100 g)		
		0	3.5	7
Visual appearance				
Color	L*	89.54 ± 0.42[a]	85.24 ± 0.56[b]	82.92 ± 0.17[c]
	a*	−2.94 ± 0.15[c]	−1.41 ± 0.22[b]	−0.27 ± 0.26[a]
	b*	10.23 ± 1.04[b]	14.30 ± 0.22[a]	14.54 ± 0.48[a]
Moisture (g/100 g wm)		67.51 ± 1.73[a]	66.62 ± 1.35[a]	65.11 ± 1.20[a]
Lipid (g/100 g dm)		17.18 ± 1.95[a]	15.73 ± 1.98[ab]	14.02± 1.55[b]
Fiber (g/100 g dm)		nd	8.81 ± 0.52[b]	16.85 ± 0.57[a]
Protein (g/100 g dm)		59.25 ± 1.66[a]	53.77 ± 1.68[b]	49.26 ± 1.77[c]
Carbohydrates* (g/100 g dm)		16.45 ± 1.86[a]	15.86 ± 0.28[a]	14.65 ± 0.15[b]
Ashes (g/100 g dm)		7.11 ± 0.57[a]	6.51 ± 0.45[a]	5.37 ± 0.44b
a_w		0.982 ± 0.005[a]	0.968 ± 0.002[b]	0.981 ± 0.002[a]
pH		4.95 ± 0.07[b]	5.16 ± 0.06[a]	5.13 ± 0.10[a]
Syneresis (%)		12.48 ± 0.91[a]	12.52 ± 2.45[a]	15.73 ± 2.98[a]

[a-c] Different letters in the same row indicate statistically different means ($p < 0.05$; ANOVA or KW). nd: not detected; wm: wet matter; dm: dry matter. *obtained by difference from other components.

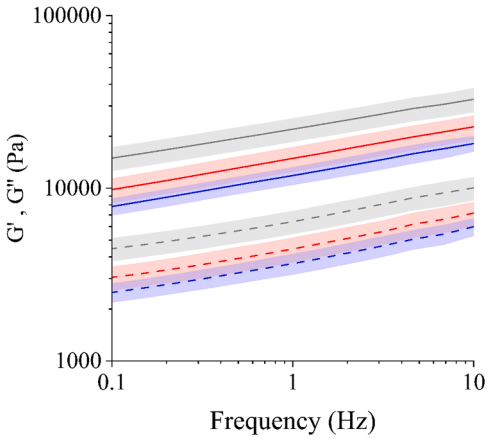

Fig. 1. Evolution of the storage modulus G' (solid lines) and the loss modulus G'' (dashed lines) as a function of oscillatory frequency relevant to samples containing 0, 3.5, and 7 g/100 g OS (light gray, red, and blue, respectively). Error bands relevant to the standard deviation of each curve are also shown.

control sample exhibits a significantly ($p < 0.05$, ANOVA) higher storage modulus (G') compared to the other spreadable cheese samples. The elastic component decreases progressively with increasing OS powder content. This trend suggests that the control sample stored a greater amount of energy during oscillatory deformation, due to the higher number of elastic interactions present in the microstructure in comparison with enriched samples. Regarding tan δ, all cheese samples exhibit a solid-like behavior typical of elastic solid materials. However, the slight increase ($p < 0.05$, KW) in tan δ with the addition of OS powders suggests a more liquid-like behavior of enriched cheeses compared to the control ones. The complex viscosity (η*) provides a measure of the material's overall resistance to flow under oscillatory shear. Data reported in Table 3 indicate that the control sample exhibits the highest η* value, which decreases with increasing OS powder content into the formulation. This reduction in complex viscosity suggests reduced intermolecular interactions and a less continuous matrix, resulting in a structure that is less capable of maintaining its integrity under applied stress. The incorporation of OS powder likely interfered with protein–protein and protein–fat interactions, resulting in a structure that is more deformable and susceptible to flow. A softening of the structure was also observed by Gammariello et al. (2008) upon the addition of insoluble chitosan in spreadable cheese samples.

The spreadability of cheese samples was then considered due to its

Table 3
Rheological parameters measured at 1 Hz and spreadability results relevant to spreadable cheese samples containing increasing amounts (0–7 g/100 g) of OS powder.

OS powder content (g/100 g)	Rheological parameters			Spreadability					
	G' (kPa)	tan δ (-)	η* (kPa·s)	Area under curve (N mm)	Peak force (N)	a (N)	b (N s^{-c}) · 10^4	c (-)	Average R^2 (-)
0	22.0 ± 4.3[a]	0.292 ± 0.001[b]	3.6 ± 0.7[a]	91.6 ± 9.1[a]	21.9 ± 1.8[a]	0.43 ± 0.07[a]	1.85 ± 0.71[a]	3.87 ± 0.15[a]	0.994
3.5	14.9 ± 2.8[b]	0.299 ± 0.001[a]	2.5 ± 0.5[b]	70.7 ± 3.7[b]	17.4 ± 1.1[b]	0.28 ± 0.04[b]	0.92 ± 0.22[ab]	4.04 ± 0.10[a]	0.996
7	11.8 ± 1.7[b]	0.309 ± 0.008[a]	2.0 ± 0.3[b]	60.4 ± 7.0[b]	14.4 ± 1.6[c]	0.24 ± 0.04[b]	1.08 ± 0.54[b]	3.96 ± 0.16[a]	0.996

[a-c] Different letters in the same row indicate statistically different means ($p < 0.05$; ANOVA or KW). Abbreviations = G': Storage modulus; tan δ: loss tangent; η*: complex viscosity; a, b, c: power law model parameters extrapolated by spreadability curves.

relevance for consumer acceptability (Fig. 2).

Data reported in Fig. 2 clearly highlighted all samples to be easily spreadable, as force curves showed profiles similar to the ones previously reported by Bayarri et al. (2012) for commercially available spreadable cheese formulations. According to Fig. 2, the addition of 3.5 and 7 g/100 g OS caused spreadable cheese to become more easily spreadable, as the force curves progressively decreased by increasing OS content. Data were thus elaborated to extrapolate further information on the effect of OS addition on the spreadability behavior of the matrix (Table 3). Spreadability data confirmed OS addition to enhance the ease of spreadability of the cheese, as both the area under the curves (*i.e.*, work required to spread the samples) and the peak force recorded (*i.e.*, maximum force opposed by the samples to the penetration of the probe) significantly decreased ($p < 0.05$, ANOVA). Curves modelling using Eq. (2) provided further insights into the mechanism of OS-induced cheese spreadability enhancement. In particular, the parameter *a*, which is indicative of the force opposed by the samples at the beginning of the spreadability assay, significantly ($p < 0.05$, ANOVA) decreased, indicating that the weakening of the samples structure occurred upon inclusion of OS was analytically detectable even upon very small deformations of the samples. At the same time, *b* also showed a significant decrease ($p < 0.05$, ANOVA) upon OS content increase, indicating that the loss of cheese mechanical properties was proportional across the entire displacement domain considered for the spreadability analysis. Differently, no significant changes ($p > 0.05$, ANOVA) were observed in the shape of the force curves with increasing OS concentrations, with *c* values being higher than 1 in all samples, indicating that the profiles exhibit statistically identical above-linear trends.

Based on these results, more in-depth information on the structural properties of spreadable cheeses was obtained through TPA analysis (Table 4).

As shown in Table 4, the inclusion of OS powders led to significant changes in the textural parameters of spreadable cheese samples. In particular, a significant reduction ($p < 0.05$, ANOVA) in hardness was observed, with values decreasing from 5.03 N to 3.39 N with the increase of OS powder content. In fresh cheeses, hardness is mainly related to moisture content and to the protein matrix structure (Diamantino et al., 2014). Since all samples showed similar moisture content (Table 2), the inclusion of 3.5 and 7 g/100 g OS probably weakened the protein network, altering the mechanical strength of enriched samples in accordance with rheological parameters (Table 3). A reduction in the hardness of spreadable cheeses was likewise observed by Difonzo et al. (2024) and partially attributed to the presence of lignocellulosic residues that alter the structural integrity of the dairy matrix. Regarding elasticity and cohesiveness, no significant differences ($p > 0.05$, ANOVA) were observed between control and enriched samples. On the other hand, gumminess progressively and significantly decreased ($p < 0.05$, ANOVA) as the concentration of OS increased, indicating not only a softer but also a less gummy texture as compared to the control sample (Table 4). Finally, adhesiveness significantly increased ($p < 0.05$, ANOVA) following the addition of OS powder, highlighting a greater tendency of the spreadable cheese to adhere to the surface during testing compared to the control sample. In particular, the sample containing 3.5 g/100 g OS showed the highest adhesiveness value, probably due to the water-binding effect of added fibers (Table 1). The latter might compete for free water and disrupt the uniformity of the casein–fat network, making the structure stickier (Cunha et al., 2010; Szafranska et al., 2021). On the other hand, incorporating more OS fiber may dry out the dairy matrix, resulting in a slight decrease of adhesiveness, although not statistically significant.

In agreement with the data relevant to small stress deformation response and spreadability (Table 3), TPA results indicated an overall decrease in sample structural resistance with increasing OS concentrations.

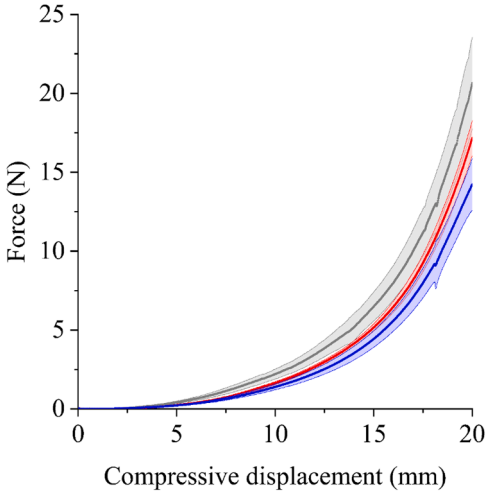

Fig. 2. Average force curves as a function of compressive displacement relevant to the spreadability assay of spreadable cheese samples containing 0, 3.5, 7 g/100 g (light gray, red, and blue, respectively) of OS powder. Error bands relevant to the standard deviation of each curve are also shown.

3.4. Microstructural properties

To better understand the microstructure of cheese samples, confocal microscopy images were acquired. In the control sample, microstructural analysis revealed a structure typical of dairy systems (Table 5). Specifically, a well-organized three-dimensional protein network (shown in purple) was clearly visible, serving as the main matrix of the system. This network efficiently incorporated the aqueous phase (black areas) thereby ensuring system stability, and also entrapped the lipid fraction, which was clearly visible as dispersed yellow droplets (Table 5).

Upon addition of 3.5 and 7 g/100 g OS powder, the insoluble fiber particles (light blue color), were observed to be heterogeneously distributed within the protein network (Table 5). These particles appeared to disrupt the continuity of the three-dimensional structure formed by proteins, thus altering its internal organization. These results were in agreement with those previously reported by Fagan et al. (2006), who observed casein coagulation to result in a much more open network upon addition of vegetable fibers like inulin, gum *acacia*, and pectin. From a mechanistic perspective, other Authors have attributed this phenomenon to the ability of casein micelles to non-covalently interact with soluble fibers, even when the latter are present at concentrations as low as 0.05 % (w/w) (Maroziene and De Kruif, 2000). In particular, even at such dilutions and at pH values close to casein isoelectric point, soluble fibers would be able to absorb on the surface of single micelles, hampering their ability to link and produce a tridimensional network. Due to these protein-soluble fiber interactions, a remarkably less cohesive protein structure was observed in the OS-enriched spreadable cheese, as evidenced by an increase in black areas (Table 5). However, the lower cohesion observed microscopically was not reflected at the macroscopic level, as the cohesiveness of the cheese samples measured by the large deformation test (Table 4) was statistically similar. Moreover, the OS powder, as shown in Table 1, exhibited a low WHC value due to their limited ability to bind water, thus acting as inactive fillers in the system not interacting with the matrix but disrupting the continuity of the casein network (Barden et al., 2015; Dickinson and Chen, 1999; Isusi et al., 2023). This reduction in the overall structural cohesion of the system was directly reflected in the loss of rheological and textural properties shown by the samples upon increasing OS content (Tables 3 and 4). Focusing the attention on the "high-fiber content" formulation (7 g/100 g OS), the micrograph reported in Table 5 highlights how OS addition not only prevented protein networking, but also significantly changed the size of the single casein

Table 4
Texture profile analysis parameters relevant to spreadable cheese samples containing increasing amounts (0–7 g/100 g) of OS powder.

OS powder content (g/100 g)	Hardness (N)	Elasticity (-)	Cohesiveness (-)	Gumminess (-)	Adhesivity (N)
0	5.03 ± 0.64[a]	0.18 ± 0.01[a]	0.22 ± 0.01[a]	1.12 ± 0.08[a]	−1.37 ± 0.34[a]
3.5	4.26 ± 0.24[b]	0.22 ± 0.02[a]	0.24 ± 0.03[a]	1.02 ± 0.16[ab]	−5.33 ± 0.68[b]
7	3.39 ± 0.75[c]	0.21 ± 0.01[a]	0.25 ± 0.02[a]	0.83 ± 0.12[b]	−3.16 ± 0.83[b]

[a-c] Different letters in the same column indicate significantly different means ($p < 0.05$, ANOVA).

Table 5
Confocal laser scanning micrographs of cheese samples, stained with Nile Red (yellow), Fast Green (purple), and Brightener (light blue) to visualize lipids, proteins, and fibers, respectively. Scale bar: 100 μm.

OS powder content (g/100 g)	Micrograph
0	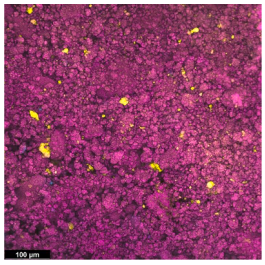
3.5	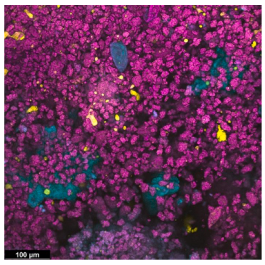
7	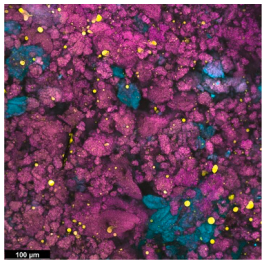

aggregates, which resulted significantly larger as compared to those present in the "fiber source" formulation (3.5 g/100 g OS) (Table 5). Despite the mechanism underlying such further modification of the cheese structure induced by high OS content, it is likely that such phenomenon was at the basis of the further decrease in rheological indices and texture observed for this specific sample (Tables 3 and 4).

Different from the protein matrix, the lipid phase appeared to be well distributed within the matrix in all samples, regardless of OS addition (Table 5).

Overall, the microstructural changes observed are consistent with the analytical results and help explain the modifications in the cheese's physical properties, particularly the increase in spreadability, reduction in rheological parameters, and variations in TPA parameters.

3.5. Sensory acceptability

A consumer test was used to evaluate the acceptance of spreadable cheese samples. In Table 6, the acceptability scores attributed by consumers to odor, taste, texture, visual appearance, and overall acceptability of samples are reported.

Table 6
Acceptability of sensory attributes (visual appearance, odor, taste, texture, overall acceptability) of control and enriched samples with OS powder (3.5 and 7 g/100 g).

OS powder content (g/100 g)	Visual appearance	Odor	Taste	Texture	Overall acceptability
0	6.53 ± 1.93[a]	6.42 ± 1.85[a]	5.88 ± 1.78[a]	4.91 ± 1.95[a]	5.70± 1.74[a]
3.5	5.93 ± 1.91[ab]	6.47 ± 2.02[a]	5.02 ± 1.95[ab]	3.65 ± 1.80[b]	4.67 ± 1.61[b]
7	5.28 ± 1.71[b]	5.95 ± 1.90[a]	4.35 ± 2.06[b]	2.93 ± 1.65[b]	3.91 ± 1.67[b]

[a-b] Different letters in the same column indicate significantly different means ($p < 0.05$, ANOVA).

Regarding the visual appearance, the control sample received the highest score, whereas the sample enriched with 7 g/100 g OS had the lowest score. This result suggested that the presence of a high amount of OS particles adversely affected consumer visual perception of the cheese. Odor ratings did not significantly differ ($p > 0.05$, ANOVA) among samples, indicating that the addition of OS powder had no notable impact on this attribute. In terms of taste, the control sample was rated as the most acceptable, while both experimental formulations received lower scores. Cheese texture was the parameter that exhibited the most pronounced differences. Specifically, the acceptability of texture decreased as the percentage of olive stone powder increased, with the most notable difference observed between the control sample and the sample containing 7 g/100 g OS, whereas no differences between the two experimental samples were detected (Table 6). The presence of insoluble dietary fiber into the cheese affected the textural mouthfeel sensation perceived by consumers, leading to prominent particle-related sensory attributes, such as chalkiness, dryness and particle perception (Chakraborty et al., 2019; Lucera et al., 2018). The control sample received the highest overall acceptability score, reflecting its more attractive sensory profile. The sample containing 3.5 g/100 g OS registered a higher overall acceptability value than the sample enriched with 7 g/100 g. Overall, these outcomes indicate that, although the incorporation of olive stone powder alters the sensory profile of samples, its use remains feasible, enhancing the nutritional value and structural characteristics of spreadable cheeses while opening new opportunities for the valorization of this by-product.

4. Conclusions

In this research, innovative spreadable cheeses enriched with OS powder were developed to valorize an underutilized resource rich in dietary fiber, meeting the criteria for both "source of fiber" and "high in fiber" nutritional claims. However, the incorporation of high value-added OS in sample formulations is not without consequences on structural and sensorial properties of cheeses. Both OS additions resulted in less elastic and softer samples due to the presence of insoluble fiber particles, which disrupted the integrity of the three-dimensional casein network. The inability of OS powder to interact with the matrix constituents led to a loss in the cohesiveness of the system at a microscopic level, therefore improving cheese spreadability. Upon sensory analysis, consumer acceptability of samples was in any case high but decreased as

the OS concentration increased, especially for the texture attribute, in which consumers were negatively influenced by the presence of insoluble particles. Generally, sensory modifications induced by OS fibers do not compromise the overall feasibility of incorporating the 3.5 g/100 g OS powder into spreadable cheese, while simultaneously enhancing its spreadability and nutritional profile. The recovery of OS in the development of fiber-enriched products might represent a pioneering way for the valorization of this by-product.

Further studies should be carried out to optimize spreadable cheese formulation and enhance consumer attractiveness, including the possibility of reducing OS particle size to potentially improve the dispersibility of insoluble fibers within the protein matrix.

Ethical statement

The authors declare that the study complied with the principles established by the Declaration of Helsinki and the protocol was approved by the Institutional Review Board of the Department of Agricultural, Food, Environmental and Animal Sciences of the University of Udine (protocol n. 0154557).

CRediT authorship contribution statement

Niccolò Renoldi: Writing – review & editing, Writing – original draft, Visualization, Methodology, Investigation, Data curation. **Federico Basso:** Writing – review & editing, Methodology, Investigation, Data curation. **Francesca Trevisiol:** Writing – review & editing, Investigation, Formal analysis. **Hana Maalej:** Writing – review & editing, Project administration. **Nadia Innocente:** Writing – review & editing, Conceptualization. **Sonia Calligaris:** Writing – review & editing, Visualization, Supervision, Project administration, Conceptualization.

Declaration of competing interest

The authors declare that they have no known competing financial interests or personal relationships that could have appeared to influence the work reported in this paper.

Acknowledgements

This research was conducted within the framework of the VALOstones project (Grant Agreement No 1837), funded by National Funding Agencies from France (French National Research Agency– ANR), Tunisia (Ministry of Higher Education and Scientific Research – MHESR), Italy (Ministry of Universities and Research – MUR), Türkiye (Scientific and Technological Research Council of Türkiye – TÜBITAK), and Morocco (Ministry of Higher Education, Scientific Research and Innovation – MESRSI). The project is supported under the Partnership for Research and Innovation in the Mediterranean Area (PRIMA), and co-funded by the European Union's Horizon 2020 Framework Programme for Research and Innovation.

The Authors would like to express their gratitude to Ms. Victoria Smilijanova for the help provided in carrying out the experimental work.

Data availability

Data will be made available on request.

References

Anderson, J.W., Baird, P., Davis, R.H., Ferreri, S., Knudtson, M., Koraym, A., Waters, V., Williams, C.L., 2009. Health benefits of dietary fiber. Nutr. Rev. 67 (4), 188–205. https://doi.org/10.1111/j.1753-4887.2009.00189.x.

AOAC, 1923. Official Methods of Analysis of the Association of Official Analytical Chemists, 7th edn. AOAC International, Gaithersburg, MD, USA.

AOAC, 2005. Official Methods of Analysis of the Association of Official Analytical Chemists, 18th edn. AOAC International, Gaithersburg, MD, USA.

AOAC, 2011. Official Methods of Analysis of the Association of Official Analytical Chemists, 18th edn. AOAC International, Gaithersburg, MD, USA.

Bai, Y., Arulrajah, A., Horpibulsuk, S., Chu, J., 2023. Gasified olive stone biochar as a green construction fill material. Constr. Build. Mater. 403, 133003. https://doi.org/10.1016/j.conbuildmat.2023.133003.

Barden, L.M., Osborne, J.A., McMahon, D.J., Foegeding, E.A., 2015. Investigating the filled gel model in Cheddar cheese through use of Sephadex beads. J. Dairy Sci. 98 (3), 1502–1516. https://doi.org/10.3168/jds.2014-8597.

Bayarri, S., Carbonell, I., Costell, E., 2012. Viscoelasticity and texture of spreadable cheeses with different fat contents at refrigeration and room temperatures. J. Dairy Sci. 95 (12), 6926–6936. https://doi.org/10.3168/jds.2012-5711.

Bolek, S., 2020. Olive stone powder: a potential source of fiber and antioxidant and its effect on the rheological characteristics of biscuit dough and quality. Innov. Food Sci. Emerg. Technol. 64, 102423. https://doi.org/10.1016/j.ifset.2020.102423.

Borneo, R., León, A.E., 2012. Whole grain cereals: functional components and health benefits. Food Funct. 3, 110–119. https://doi.org/10.1039/c1fo10165j.

Bouchelta, C., Medjram, M.S., Bertrand, O., Bellat, J.P., 2008. Preparation and characterization of activated carbon from date stones by physical activation with steam. J. Anal. Appl. Pyrolysis. 82 (1), 70–77. https://doi.org/10.1016/j.jaap.2007.12.009.

Brummer, Y., Kaviani, M., Tosh, S.M., 2015. Structural and functional characteristics of dietary fibre in beans, lentils, peas and chickpeas. Food Res. Int. 67, 117–125. https://doi.org/10.1016/j.foodres.2014.11.009.

Chakraborty, P., Witt, T., Harris, D., Ashton, J., Stokes, J.R., Smyth, H.E., 2019. Texture and mouthfeel perceptions of a model beverage system containing soluble and insoluble oat bran fibres. Food Res. Int. 120, 62–72. https://doi.org/10.1016/j.foodres.2019.01.070.

Cunha, C.R., Dias, A.I., Viotto, W.H., 2010. Microstructure, texture, colour and sensory evaluation of a spreadable processed cheese analogue made with vegetable fat. Food Res. Int. 43, 723–729. https://doi.org/10.1016/j.foodres.2009.11.009.

de Oliveira Menali, L., Zidanes, U.L., Dias, M.C., Setter, C., Silveira, M.N.L., Faria, D.L., Mori, F.A., Júnior, J.B.G., Ferreira, S.R., 2024. Production and analysis of the physical and mechanical of particleboards panels produced with Acrocomia aculeata endocarp. Cerne 30 (1), 1–15. https://doi.org/10.1590/01047760202430013302.

Dewi, K.S., Gavahian, M., Phimolsiripol, Y., 2025. Dietary fiber supplementation in animal products: recent developments, commercial applications, and sustainability impact. Food Biosci. 68, 106668. https://doi.org/10.1016/j.fbio.2025.106668.

Diamantino, V.R., Beraldo, F.A., Sunakozawa, T.N., Penna, A.L.B., 2014. Effect of octenyl succinylated waxy starch as a fat mimetic on texture, microstructure and physicochemical properties of Minas fresh cheese. LWT 56 (2), 356–362. https://doi.org/10.1016/j.lwt.2013.12.001.

Dickinson, E., Chen, J., 1999. Heat-set whey protein emulsion gels: role of active and inactive filler particles. J. Dispers. Sci. Technol. 20 (1–2), 197–213. https://doi.org/10.1080/01932699908943787.

Difonzo, G., Antonino, C., Caponio, G.R., Vacca, M., Liuzzi, F., De Bari, I., Valerio, V., Faccia, M., De Angelis, M., 2024. Enhanced production of xylooligosaccharides from vine shoots and their impact on the nutritional and technological properties of spreadable goat cheese. LWT 206, 116605. https://doi.org/10.1016/j.lwt.2024.116605.

EFSA, 2016. Scientific opinion on dietary reference values for carbohydrates and dietary fibre. EFSA J. 8 (3), 1–77. https://doi.org/10.2903/j.efsa.2010.1462.

European Parliament and Council, 2006. Regulation (EC) No 1924/2006 of the European parliament and the of the council on nutrition and health claims made on foods. OJ 404, 9–25.

Faber, T.J., Jaishankar, A., McKinley, G.H., 2017. Describing the firmness, springiness and rubberiness of food gels using fractional calculus. Part II: measurements on semi-hard cheese. Food Hydrocoll. 62, 325–339. https://doi.org/10.1016/j.foodhyd.2016.06.038.

Fagan, C.C., O'Donnell, C.P., Cullen, P.J., Brennan, C.S., 2006. The effect of dietary fibre inclusion on milk coagulation kinetics. J. Food Eng. 77 (2), 261–268. https://doi.org/10.1016/j.jfoodeng.2005.06.030.

Gammariello, D., Chillo, S., Mastromatteo, M., Di Giulio, S., Attanasio, M., Del Nobile, M. A., 2008. Effect of chitosan on the rheological and sensorial characteristics of apulia spreadable cheese. J. Dairy Sci. 91 (11), 4155–4163. https://doi.org/10.3168/jds.2008-1280.

García Martín, J.F., Cuevas, M., Feng, C., Mateos, P.Á., Torres, M., 2020. Energetic valorisation of olive biomass: olive-tree. Processes 8 (511), 1–38.

Gomes, E.R., Barroso dos Anjos Pinto, C., Stephani, R., Fernandes de Carvalho, A., Perrone, Í.T., 2023. Effect of adding different types of soluble fibre to high-protein yoghurts on water holding capacity, particle size distribution, apparent viscosity, and microstructure. Int. Dairy J. 141, 105609. https://doi.org/10.1016/j.idairyj.2023.105609.

Hannachi, H., Elfalleh, W., Laajel, M., Ennajeh, I., Mechlouch, R.F., Nagaz, K., 2020. Chemical profiles and antioxidant activities of leaf, pulp, and stone of cultivated and wild olive trees (Olea Europaea L.). Int. J. Fruit Sci. 20 (3), 350–370. https://doi.org/10.1080/15538362.2019.1644574.

Heuscher, S.A., Brandt, C.C., Jardine, P.M., 2005. Using soil physical and chemical properties to estimate bulk density. Soil Sci. Soc. Am. J. 69 (1), 51–56. https://doi.org/10.2136/sssaj2005.0051a.

IDF, 2011. Cheese and Processed Cheese – Determination of the Nitrogenous Fractions, 224. International Dairy Federation Standard FIL-IDF, Brussels, Belgium, 2011.

IDF, 2021. Cheese – Guidance on Sample Preparation For Physical and Chemical Testing, 224. International Dairy Federation Standard FIL-IDF, Brussels, Belgium, 2011.

IDF, 2022. Cheese and Processed Cheese products, Caseins and Caseinates – Determination of Fat Content – Gravimetric method, 250. International Dairy Federation Standard FIL-IDF, Brussels, Belgium, 2022.

Isusi, G.I.S., Marburger, J., Lohner, N., van der Schaaf, U.S., 2023. Texturing of soy yoghurt alternatives: pectin microgel particles serve as inactive fillers and weaken the soy protein gel structure. Gels 9 (6). https://doi.org/10.3390/gels9060473.

Jahanbakhshi, R., Ansari, S., 2020. Physicochemical properties of sponge cake fortified by olive stone powder. J. Food Qual. 1–11. https://doi.org/10.1155/2020/1493638.

Leach, M.R., Farkas, B.E., Daubert, C.R., 2003. Rheological characterization of process cheese using tube viscometry. Int. J. Food Prop. 6 (2), 259–267. https://doi.org/10.1081/JFP-120017847.

Lucera, A., Costa, C., Marinelli, V., Saccotelli, M.A., Del Nobile, M.A., Conte, A., 2018. Fruit and vegetable by-products to fortify spreadable cheese. Antioxidants 7 (5), 1–10. https://doi.org/10.3390/antiox7050061.

Manzocco, L., Barozzi, L., Plazzotta, S., Sun, Y., Miao, S., Calligaris, S., 2024. Feasibility of water-to-ethanol solvent exchange combined with supercritical CO2 drying to turn pea waste into food powders with target technological and sensory properties. LWT 194, 115778. https://doi.org/10.1016/j.lwt.2024.115778.

Maroziene, A., De Kruif, C.G., 2000. Interaction of pectin and casein micelles. Food Hydrocoll 14 (4), 391–394. https://doi.org/10.1016/S0268-005X(00)00019-9.

Monteiro, R.R., Tavares, D.Q., Kindstedt, P.S., Gigante, M.L., 2009. Effect of pH on microstructure and characteristics of cream cheese. J. Food Sci. 74 (2), 112–117. https://doi.org/10.1111/j.1750-3841.2008.01037.x.

Mudgil, D. Barak, S., 2013. Composition, properties and health benefits of indigestible carbohydrate polymers as dietary fiber: A review. Int. J. Biol. Macromol. 61, 1-6. 10.1016/j.ijbiomac.2013.06.044.

Oncel, B., Ozbek, C., 2025. Optimization of olive stone powder tea production: infusion conditions, bioactive compounds, and sensory evaluation using response surface method. J. Food Meas. Charact. 19, 4278–4291. https://doi.org/10.1007/s11694-025-03252-3.

Rao, M.A., Steffe, J.F., 1992. Viscoelastic Properties of Foods. Elsevier Applied Science, New York, NY.

Renoldi, N., Melchior, S., Calligaris, S., Peressini, D., 2023. Application of high-pressure homogenization to steer the technological functionalities of chia fibre-protein concentrate. Food Hydrocoll. 139, 108505. https://doi.org/10.1016/j.foodhyd.2023.108505.

Rezvani, Z., Goli, S.A.H., 2024. Production of milk-based drink enriched by dietary fiber using carrot pomace: physicochemical and organoleptic properties during storage. Food Hydrocoll. 151, 109834. https://doi.org/10.1016/j.foodhyd.2024.109834.

Rinaldoni, A.N., Palatnik, D.R., Zaritzky, N., Campderrós, M.E., 2014. Soft cheese-like product development enriched with soy protein concentrates. LWT 55 (1), 139–147. https://doi.org/10.1016/j.lwt.2013.09.003.

Slavin, J.L., Lloyd, B., 2012. Health benefits of fruits and vegetables. Adv. Nutr. 3, 506–516. https://doi.org/10.3945/an.112.002154.

Soares, T.F., Alves, R.C., Oliveira, M.B.P.P., 2024. From olive oil production to by-products: emergent technologies to extract bioactive compounds. Food Rev. Int. 40 (10), 3342–3369. https://doi.org/10.1080/87559129.2024.2354331.

Szafranska, J.O., Muszynski, S., Tomasevic, I., Sołowiej, B.G., 2021. The influence of dietary fibers on physicochemical properties of acid casein processed cheese sauces obtained with whey proteins and coconut oil or anhydrous milk fat. Foods 10 (759), 1–21. https://doi.org/10.3390/foods10040759.

Tian, Y., Sheng, Y., Wu, T., Wang, C., 2024. Effect of modified okara insoluble dietary fibre on the quality of yoghurt. Food Chem. 21, 101064. https://doi.org/10.1016/j.fochx.2023.101064.

Tolve, R., Zanoni, M., Ferrentino, G., Gonzalez-Ortega, R., Sportiello, L., Scampicchio, M., Favati, F., 2024. Dietary fibers effects on physical, thermal, and sensory properties of low-fat ice cream. LWT 199, 116094. https://doi.org/10.1016/j.lwt.2024.116094.

Trumbo, P., Schllicker, S., Yates, A.A., Poos, M., 2002. Dietary reference intakes for energy, carbohydrate, Fiber, fat, fatty acids, cholesterol, protein and amino acids. J. Am. Diet. Assoc. 102 (11), 1621–1630. https://doi.org/10.1016/S0002-8223(02)90346-9.

Zhao, L., Zhang, F., Ding, X., Wu, G., Lam, Y.Y., Wang, X., Fu, H., Xue, X., Lu, C., Ma, J., Yu, L., Xu, C., Ren, Z., Xu, Y., Xu, S., Shen, H., Zhu, X., Shi, Y., Shen, Q., Zhang, C., 2018. Gut bacteria selectively promoted by dietary fibers alleviate type 2 diabetes. Science 359, 1151–1156. https://doi.org/10.1126/science.aao5774.